JOURNAL OF CATALYSIS 96, 507–516 (1985)

Reaction Kinetics of Methylcyclohexane Dehydrogenation over a Sulfided Pt + Re/Al_2O_3 Reforming Catalyst

MICHAEL A. PACHECO[1] AND EUGENE E. PETERSEN

Department of Chemical Engineering, University of California, Berkeley, California 94720

Received June 4, 1984; revised June 18, 1985

An investigation of the reaction kinetics of methylcyclohexane (MCH) dehydrogenation over a sulfided Pt + Re/Al_2O_3 reforming catalyst is presented. The main reaction kinetics cannot be modeled completely with simple Langmuir–Hinshelwood techniques. The main reaction appears to be controlled by adsorption of reactant and occurs as a consecutive series of steps, with methylcyclohexene as an observable intermediate. The fouling reaction is observed to be first order in MCH and toluene, and inhibited by hydrogen. The activation energy of the main reaction (14 kcal/mol) and the fouling reaction (78 kcal/mol) are very similar to the same for an unsulfided Pt/Al_2O_3 catalyst. The results are interpreted in terms of a recently proposed fouling model and suggest that the active sites of the sulfided bimetallic are partitioned into very small ensembles.

INTRODUCTION

The Pt + Re/Al_2O_3 naphtha reforming catalyst (*1*) has received much attention since its discovery. A better understanding of the role of rhenium in this catalyst may lead to the development of even better catalysts.

Of all the publications pertaining to the Pt + Re/Al_2O_3 catalyst, there are few, if any, fundamental investigations into the kinetics of a model reforming reaction over this catalyst. The results of an extensive kinetics study of a model reaction and the accompanying fouling reaction over this catalyst are presented herein. The model reaction is the dehydrogenation of methylcyclohexane (MCH) to toluene.

There is very little improvement in the stability of the bimetallic (Pt + Re) over the monometallic (Pt) catalyst without presulfiding. Therefore, to make this work more relevant, this study involves the sulfided bimetallic catalyst exclusively.

This work was initiated primarily to investigate the stabilizing role of rhenium in the sulfided bimetallic catalyst. In order to accomplish this, both the main and fouling reaction kinetics of MCH dehydrogenation over the sulfided Pt + Re catalyst were studied. The kinetics of this model reaction system have already been established for an unsulfided Pt/Al_2O_3 catalyst (*2, 3*). A comparison of the results for the two catalysts provides some insight into the role of rhenium and sulfur in the bimetallic catalyst.

EXPERIMENTAL

(*1*) *Reactor System*

An external recycle reactor with a variable space velocity was used for this study. The reactor and all the peripherals are described elsewhere (*4*). The major components of the system and their operation are unchanged from the earlier work, unless specified otherwise. The reactor has a nominal residence time of 3 s, operates with a recycle ratio in excess of 10/1, and employs a nominal particle size of 80 μm. This setup allows the acquisition of fundamental data on rapidly deactivating catalysts in the absence of mass transfer effects.

[1] Present address: AMOCO Oil Co., P.O. Box 400, Naperville, Ill. 60566.

0021-9517/85 $3.00

(2) Materials

The reactant feedstock for all experiments is Kodak spectroquality MCH. The carrier gases are Matheson UHP hydrogen (99.999%) and distilled helium (99.995%). The catalyst was generously donated by Chevron Research Company and is nominally 0.3 wt% Pt, 0.3 wt% Re, and 0.6 wt% Cl on γ-Al_2O_3. The surface area of the support is nominally 200 m^2/g.

(3) Gas Analysis

The reactor feed and product streams were quantitatively analyzed in order to determine the reaction rate and selectivity. All analyses were performed by an on-line Varian 1520 gas chromatograph. A $\frac{1}{8}$-in. × 12-foot S.S. column packed with 15% DEGS on Chromosorb W was used with a flame-ionization detector (FID).

The output from the GC was digitized and the data stored on floppy diskettes. Following the elution of the sample, the chromatogram was interpreted by a BASIC computer program. The program was custom designed for these chromatograms. It locates the GC peaks and numerically determines the peak areas using the trapezoidal rule.

The A/D conversion was performed by a standard Keithly digital voltmeter (Model 192). The digitized signal was sent to a Commodore (PET) computer via the IEEE/488 interface.

Compound identification was routinely performed simply by retention time alone. On some early experiments, these identifications were checked and verified by an off-line GC/MS analysis of "gas bomb" samples.

(4) Catalyst Pretreatment

Prior to all kinetic studies, the catalyst was exposed to the following *in situ* pretreatment. The catalyst was heated from room temperature to 500°C over a 1.5-h period and held at this temperature for 4 h. During this heat-up and calcination, the catalyst loading (20–120 mg) was held in a flowing stream of gas composed of 100 Torr O_2 and 700 Torr N_2 (300 cm^3/m at RTP). The catalyst was then cooled to 360°C over 2 h. During this cool-down, the reactor was purged with a flowing stream of helium (300 cm^3/min at RTP). The catalyst was then reduced in flowing hydrogen for 15 h at 360°C (200 cm^3/m at RTP).

Following reduction, the catalyst was subjected to the following "standard" sulfiding treatment. The catalyst temperature was raised to 500°C over a 40-min period. During this heat-up period, the reactor was held in flowing hydrogen (200 cm^3/m at RTP). The catalyst was exposed to 5 atoms of sulfur per Pt atom at 500°C. The exposure was accomplished by introducing 3-ml aliquots of 1000 ppm H_2S (in hydrogen) into the flowing stream of hydrogen (200 cm^3/m at RTP). The aliquots of H_2S were introduced at 1-min intervals. Immediately after the sulfiding treatment, the reactor was cooled to 360°C and held overnight (~16 h) in flowing hydrogen (200 cm^3/m at RTP). Previous sulfiding experiments (*5*) indicate this pretreatment gives a reproducible and irreversibly sulfided state of the catalyst.

(5) Initial Rate Experiments

In order to study the effect of process variables on the main reaction rate, an extensive set of reaction rate data was obtained on the unfouled catalyst. The catalyst was typically held in flowing hydrogen for several days during which time intermittent experiments were performed. These experiments consisted of introducing a stable feed mixture (analyzed by GC) to replace the flowing hydrogen. After 15 s, the reactor was essentially at steady state and a product sample was automatically injected into the GC for analysis. The feed mixture was then immediately replaced by the original flowing hydrogen stream.

From the feed and product analyses and the measured space velocity, the reaction rate can be determined. It is assumed that any fouling that occurs during these tests is

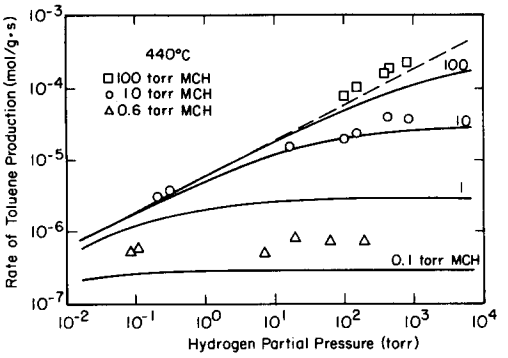

FIG. 1. The effect of MCH and H_2 on the rate of toluene production. Solid lines represent Eq. (1).

completely reversible in the flowing hydrogen stream. At least 20 min recovery time elapsed between each experiment.

(6) *Fouling Experiments*

The operational policy of the gradientless reactor has been described previously (*4*). It is only important to highlight some key aspects for the purpose of this paper.

The concentration of the product (toluene) is continuously monitored by means of an on-line IR spectrometer. This measurement is held constant as the catalyst deactivates by varying the space velocity to just compensate for the loss in activity. Periodic GC analyses of reactor effluent and feed streams along with the measured reaction temperature, pressure, and space velocity provide the reaction rate versus time data (at constant conversion).

RESULTS

(1) *Main Reaction*

The kinetics for the conversion of MCH to toluene are summarized in Figs. 1 through 3. This reaction appears to exhibit several different kinetic regimes for the range of conditions studied. An isothermal transition from a region characterized by +1-order MCH and zero-order H_2 kinetics to a region characterized by nearly zero-order MCH kinetics and $+\frac{1}{2}$-order H_2 kinetics is shown in Fig. 1. The kinetic rate expression shown below provides an adequate fit of the isothermal data, as shown by the solid lines in Fig. 1.

$$r_{TOL} = \frac{k_0[MCH]}{1 + K_2 \dfrac{[MCH]}{[H_2]^{1/2}}}, \qquad (1)$$

where

k_0 = 0.055 (mol/g · s · Torr) at 440°C

K_2 = 0.5 ($Torr^{-1/2}$) at 440°C

[MCH] = MCH partial pressure in reactor (Torr)

$[H_2]$ = H_2 partial pressure in reactor (Torr)

r_{TOL} = rate of production of toluene (mol/g · s).

In order to test the temperature dependence of k_0 and K_2, Arrhenius experiments were conducted in each of the two regions. Both sets of data are shown in Fig. 2. There appears to be a third kinetic region in the low MCH/high H_2 data at very low (<360°C) temperatures. This is observed from the sharp bend in these Arrhenius data (triangles) in Fig. 2. This bend cannot be

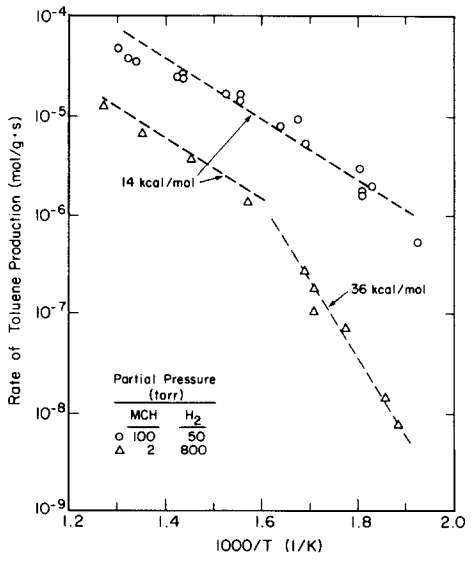

FIG. 2. The effect of temperature on the rate of toluene production.

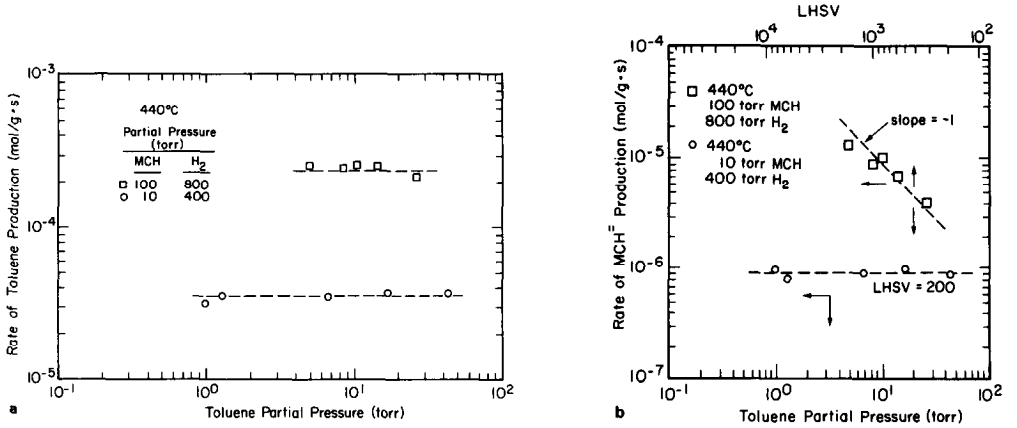

FIG. 3. The effect of toluene on the rate of (a) toluene production and (b) intermediate ($MCH^=$) production.

explained by Eq. (1). It is also noted that the high MCH/low H_2 data (circles) in Fig. 2 could easily be interpreted as a combination of more than one linear region. Again, this complication cannot be explained by Eq. (1).

In order to check for product inhibition, the effect of toluene concentration on the observed rate has been studied. This was accomplished in two ways. First, a series of initial rate experiments were conducted, all with the same space velocity of MCH (LHSV = 200). The feed was doped with varying amounts of toluene. The reaction rate did not change in response to the toluene introduced in the feed. The results of this set of experiments are shown in Fig. 3a (circles).

The second test for product inhibition was done by varying the LHSV. The concentration of MCH in the feed was adjusted slightly in conjunction with the LHSV so as to hold the MCH concentration in the reactor constant. The LHSV was varied over the range of 300 to 2000. The result of this set of experiments are also shown in Fig. 3a (squares).

From the preceding two sets of experiments it is concluded that the concentration of toluene in the reactor does not influence the initial rate of production of toluene over the sulfided bimetallic catalyst.

(2) Secondary Reaction

In addition to the primary product, toluene, a significant production of the three isomers of methylcyclohexene ($MCH^=$) was observed. All three $MCH^=$ isomers have been isolated and identified in samples of our reactor product with the off-line GC/MS. However, it is only possible to separate one of the isomers (methylcyclohex-1-ene, $MCH_1^=$) from MCH with the routine on-line GC analysis. The ratio of the area under the $MCH_1^=$ peak divided by the area under the MCH peak from the product gas analyses will be referred to as the $MCH^=$ yield. This $MCH^=$ yield is typically on the order of 10^{-3} while the toluene yield is typically on the order of 10^{-1}.

The $MCH^=$ yield is independent of all gas-phase concentrations, MCH, H_2, and toluene. It depends only on the reaction temperature of the experiment. These observations indicate that $MCH^=$ might be a gas-phase intermediate of a consecutive irreversible reaction mechanism as shown in

$$MCH \xrightarrow{k_1} MCH^= \xrightarrow{k_3} TOL. \qquad (2)$$

The reverse reactions are neglected since the equilibrium conversions are not approached in any of the studies presented herein.

If the consecutive mechanism in Reac-

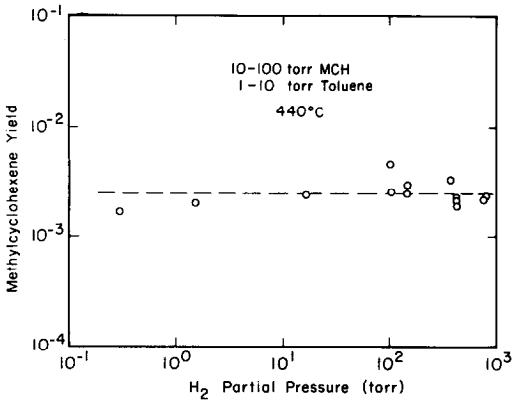

FIG. 4. The effect of H_2 on the intermediate product yield ($MCH^=$ yield).

tion (2) is correct, it follows that the rate of $MCH^=$ production should exhibit the trend observed in Fig. 3b. These data are from the same experiments presented in Fig. 3a. They demonstrate that, for a given temperature and MCH concentration in the reactor, the rate of $MCH^=$ production is independent of the toluene concentration at a constant space velocity (circles). However, the rate of $MCH^=$ production increases with space velocity and therefore can appear to depend on the toluene concentration (squares).

The invariance of the $MCH^=$ yield with respect to H_2 partial pressure shown in Fig. 4 is very important. This supports the assumption that the reverse reactions can be safely neglected under these reaction conditions.

For this reaction system, Eq. (3) can be derived by dividing the $MCH^=$ component balance by the MCH component balance for a CSTR. The second term in the brackets is on the order of 10^{-2} for this system and can therefore be neglected. This shows that the apparent activation energy of the $MCH^=$ yield in the reactor effluent is equal to the difference in activation energies of the two consecutive steps.

$$\frac{k_3}{k_1} = \frac{[MCH]}{[MCH^=]}\left[1 - \frac{[MCH^=]}{[MCH]_0 - [MCH]}\right], \quad (3)$$

where

k_1 = rate constant for first step of Reaction (2)

k_3 = rate constant for second step of Reaction (2)

$[MCH^=]$ = $MCH^=$ partial pressure in reactor (Torr)

$[MCH]_0$ = MCH partial pressure in feed (Torr).

The methylcyclohexene yield exhibits nearly the same temperature dependence as the first-order rate constant for toluene production. This indicates a very small value of the activation energy for the second step (ΔE_3). Arrhenius data for a representative group of data are shown in Figs. 5a and b. The linear slopes for these data determined by linear regression indicate that the activation energy of the second step (ΔE_3) is approximately 2 kcal/mol. The discrepancy between the 14 kcal/mol reported in Fig. 2 and the 12 kcal/mol reported in Fig. 5a is representative of the degree of reproducibility that is obtained from one catalyst loading to another.

(3) Fouling Reaction

A summary of the data for eight different catalyst deactivation experiments is shown in Fig. 6 along with a previously noted empirical correlation (*2*). The time invariant reaction conditions for these data are given in Table 1. All the data are well represented by a previously reported fundamental fouling model (*6*). For this case, the initial activity of the catalyst is well represented by a constant value of $a_0 = 0.1$ and the specific fouling rates are well represented by Eq. (4). The observed and predicted values for k_f are shown in Table 1 for the appropriate conditions.

$$(k_f)_{Bi} = 6.8 \times 10^{26} \frac{[MCH][TOL]}{[H_2]^{1.3}} \exp\{-39{,}000/T\}, \quad (4)$$

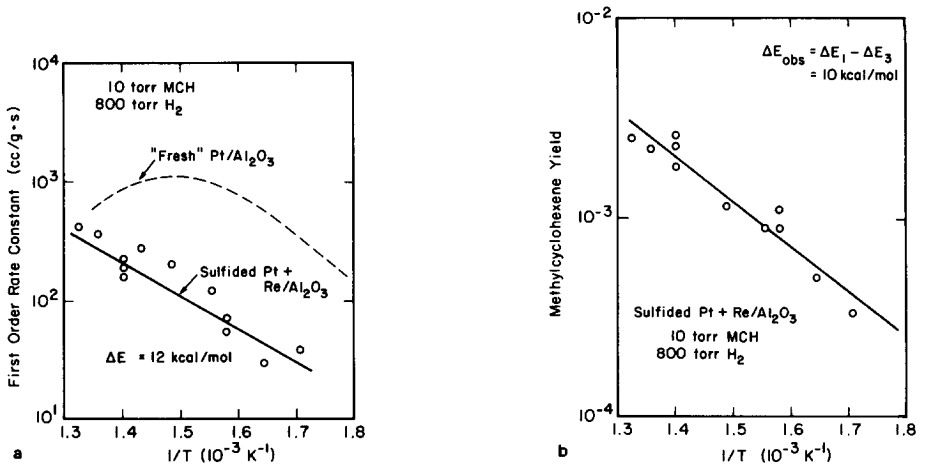

FIG. 5. Arrhenius data for (a) main reaction rate constant and (b) intermediate product yield. Activation energies pertain to Reaction (2).

where

$(k_f)_{Bi}$ ≡ specific fouling rate for the sulfided bimetallic catalyst (min^{-1})

[TOL] ≡ toluene partial pressure in reactor (Torr).

The variation of the specific fouling rate in response to the individual process variables is shown in Figs. 7 through 10. The solid line in each of these figures represents Eq. (4). The specific fouling rate data in each of these figures have been corrected to a reference condition corresponding to 10 Torr MCH, 3 Torr toluene, 400 Torr H_2, and 440°C. In each figure, the effect of a single process variable is assessed. The specific fouling rates were corrected for deviations in the other three process variables from the reference condition according to Eq. (4).

A positive dependence (~1st order) of k_f on MCH and toluene is observed in Figs. 7 and 8, respectively. A negative dependence

TABLE 1

A Summary of the Process Variables for the Sulfided Pt + Re/Al_2O_3 Catalyst Deactivation Data[a]

Run No.	Symbol	Reaction conditions				Specific fouling rate (min^{-1})	
		Temp. (°C)	Partial press. (Torr)			Observed	Predicted (Eq. (4))
			MCH	Toluene	H_2		
34	▽	425	10	3	800	2.0×10^0	1.9×10^0
44	○	440	10	3	400	1.6×10^1	1.5×10^1
43	□	440	40	3	400	6.4×10^1	6.0×10^1
58	◇	440	40	2	200	8.8×10^1	9.8×10^1
41	⊗	440	30	9	400	1.2×10^2	1.4×10^2
46	⊠	440	100	9	400	4.6×10^2	4.5×10^2
47	◆	440	10	0.1	0.3	3.2×10^3	5.7×10^3
61	△	465	100	1	50	1.0×10^4	4.7×10^3

[a] Symbols refer to those used in Fig. 6.

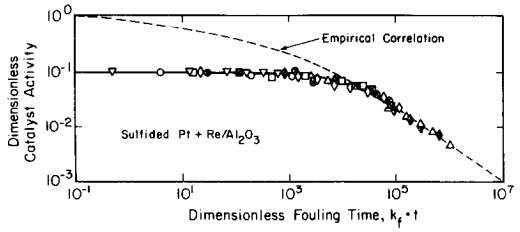

FIG. 6. Summary of catalyst fouling data for MCH dehydrogenation over a sulfided Pt + Re/Al_2O_3 catalyst. Reaction conditions and specific fouling rates are in Table 1.

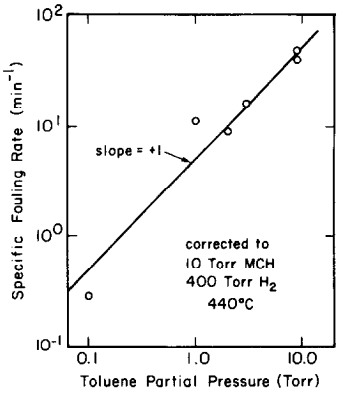

FIG. 8. Effect of toluene on the specific fouling rate for MCH dehydrogenation over sulfided Pt + Re/Al_2O_3 (solid line represents Eq. (4)).

of k_f on H_2 is observed in Fig. 9. This effect can be modeled by a constant −1.3-order simple power-law dependence. The effect of temperature follows an Arrhenius behavior with an apparent activation energy of ~78 kcal/mol as shown in Fig. 10.

DISCUSSION

There are no fundamental kinetic studies of this reaction system available for comparison. But, there are several kinetic studies of this reaction over an unsulfided Pt/Al_2O_3 catalyst (*3, 7, 8*). Much of the work is consistent with the functional form of the general rate expression in

$$r_{TOL} = \frac{k \cdot [MCH]}{\left\{1 + K_x \frac{[MCH]}{[H_2]^x} + \frac{K_y[TOL]}{H_2^y}\right\}}. \quad (5)$$

This expression can be obtained via a Langmuir–Hinshelwood derivation by assuming that adsorption of reactant is rate determining and that there are three states of the active catalyst sites: vacant sites, adsorbed reactant (MCH), and adsorbed product (TOL).

The adsorbed MCH state can be modeled as dissociative adsorption with $x = \frac{1}{2}$ as presented herein, or associative adsorption with $x = 0$ as presented elsewhere (*3, 8*). In order to be consistent with the rate-deter-

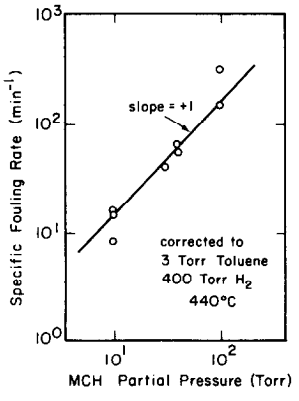

FIG. 7. Effect of MCH on the specific fouling rate for MCH dehydrogenation over sulfided Pt + Re/Al_2O_3 (solid line represents Eq. (4)).

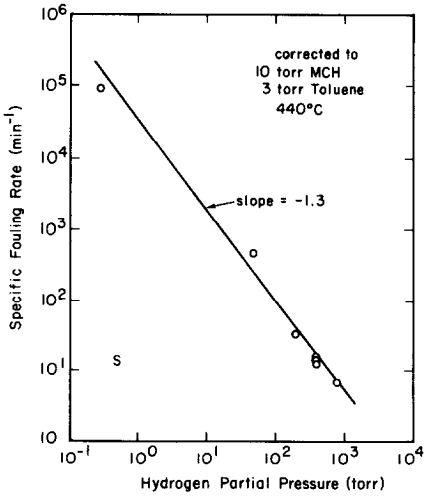

FIG. 9. Effect of H_2 on the specific fouling rate for MCH dehydrogenation over sulfided Pt + Re/Al_2O_3 (solid line represents Eq. (4)).

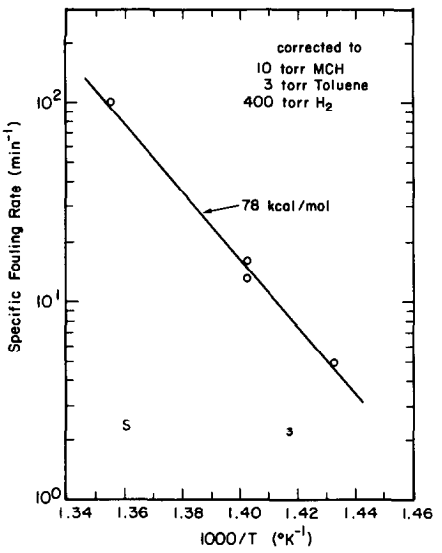

FIG. 10. Effect of temperature on the specific fouling rate for MCH dehydrogenation over sulfided Pt + Re/Al_2O_3 (solid line represents Eq. (4)).

mining step (rds), this state of adsorbed MCH must be nonproductive. For example, it may correspond to a MCH molecule adsorbed through the methyl group as discussed by others (*9*).

The adsorbed toluene state can be modeled as associative adsorption with $y = 0$ in all cases. In some work (*8*), toluene inhibition is not observed at all as is the case herein. In other work (*3, 7*), fractional order inhibition is observed. For example, the rate of toluene production has been reportedly inhibited by toluene to the $-\frac{1}{2}$ order in one case (*7*) and to the $-\frac{1}{3}$ order elsewhere (*3*). All the observations are consistent with the form of Eq. (5), so long as the terms in the denominator are of the appropriate magnitude.

It is interesting that, over the same range of conditions, toluene inhibition is observed over the unsulfided monometallic (*3*) but not over the sulfided bimetallic (Fig. 3a). This indicates that the extent of coverage by adsorbed toluene in these two systems is quite different.

The Arrhenius data for the main reaction in Fig. 2 are not adequately represented by reasonable temperature dependencies of the constants in Eq. (1) or Eq. (5). The poor linearity of the circles and the sharp kink in the triangles indicate that the model (Eq. (1)) is only an approximation of the actual data. A few preliminary experiments have indicated the sharp kink in the low MCH/high H_2 data is not due to toluene adsorption at the lower temperatures. This matter has not been pursued in any detail.

The problems encountered in trying to model the Arrhenius data in Fig. 2 are conspicuously similar to complications that can arise because of internal mass transport limitations. However, the value of the effective diffusivity required to explain the data can be easily estimated and is on the order of 6×10^{-5} cm^2/s (for the data in Fig. 2, triangles). However, studies in a single-pellet diffusion reactor indicate that the actual effective diffusivity is about 3×10^{-2} cm^2/s. Therefore, it is unlikely that mass transport limitations are important in this case.

The direction of the kink in the low MCH/high H_2 data in Fig. 2 leads one to be suspicious of equilibrium limitations at the lower temperatures. However, a careful analysis demonstrates that the observed conversions are at least two orders of magnitude lower than the equilibrium conversion, even for the lowest temperatures reported in Fig. 2. This can be determined directly from the data in Fig. 2 given that the nominal LHSV for the triangles is 10 and that for the circles is 1000. A complete summary of the exact experimental conditions for each data point in Figs. 1 through 5 is too lengthy to be presented herein, but can be found in Appendix 3 of Ref. (*12*). It is important to note in Fig. 5a that the relative maximum, previously observed for the Pt/Al_2O_3 catalyst and attributed to fouling that occurs during the reactor transient prior to steady state (*2*), is not observed in any of the experiments with the bimetallic catalyst. This is in agreement with the previously presented model (*6*) which predicts the relative maximum will be shifted to a

much higher temperature for the sulfided bimetallic.

A very small amount of benzene production is observed over this catalyst, indicating that dealkylation does occur. However, the selectivity toward this product is on the order of 10^{-4}–10^{-5}, and it was not possible to measure this low concentration of product with the on-line GC reliably.

The fouling data presented in Fig. 6 provide a demanding test of a previously reported fouling model (*6*). The data span over 6 decades of dimensionless time. All fouling experiments were conducted with a specific fouling rate sufficiently small such that no significant fouling occurs during the initial reactor transient. Therefore, all the data originate from the same plateau of initial activity.

It is most interesting to observe the utility of the fouling model (*6*) despite the shortcomings of the model for the initial rate measurements (Eq. (1)). The observed initial reaction rates for the production of toluene are difficult, if not impossible, to model with simple Langmuir–Hinshelwood techniques. However, it may be reasonable to assume that the sulfided catalyst is poisoned to the same extent at the beginning of each fouling experiment. All the fouling data can be successfully modeled on the basis of a constant initial activity of 0.1. The 10% activity level is consistent with a comparative study between this catalyst and the monometallic Pt/Al_2O_3 (*11*).

The specific fouling rates used to nondimensionalize time were presented in Table 1. These values are constant over the entire length of the experiment because the reaction environment is held constant by adjusting the space velocity with time. These constants are determined by utilizing the properties of a logarithmic coordinate system. This is accomplished by simply matching the shape of the empirical fouling data to the previously observed dimensionless fouling correlation (*2*).

In previous work (*2, 6*), the fouling of a monometallic Pt/Al_2O_3 catalyst accompanying the dehydrogenation of MCH has been modeled. A Rideal–Eley type of mechanism was proposed, gas-phase toluene reacting with adsorbed MCH was the rds. The number of sites involved in the adsorbed reactant varied as the catalyst deactivated. A model based on a simple sextet of sites was successful for catalyst activities above about 40%. The functional dependence of the specific fouling rate on the process variables for the unsulfided Pt/Al_2O_3 catalyst is well represented by

$$(k_f)_{mono} = 1.3 \times 10^{40} \frac{[MCH]}{[TOL][H_2]^{5.5}} \exp\{-37{,}000/T\}, \quad (6)$$

where

$(k_f)_{mono} \equiv$ specific fouling rate for the unsulfided monometallic catalyst (min^{-1}).

It is interesting to compare the result for the sulfided bimetallic catalyst (Eq. (4)) with the result for the unsulfided monometallic catalyst (Eq. (6)). A very different toluence dependence is observed: -1 order for Pt/Al_2O_3 versus $+1$ order for sulfided Pt + Re/Al_2O_3. In view of the differences in the main reaction kinetics, this difference is not surprising. The toluene inhibition of the fouling reaction (shown in Eq. (6)) was attributed to a relatively high degree of surface coverage by adsorbed toluene (*2*). It is consistent with the fractional order toluene inhibition of the main reaction (*3*). However, in the case of the sulfided bimetallic, no such inhibition is observed for the main reaction (Fig. 3a) as well as the fouling reaction (Fig. 8). This is a further indication that the extent of coverage by adsorbed toluene in these two systems is significantly different.

Another very interesting difference is the observed hydrogen dependence: -5.5 order for Pt/Al_2O_3 versus -1.3 order for sulfided Pt +Re/Al_2O_3. This difference is a little more difficult to explain. If fewer sites are involved in the rds of the fouling pro-

cess, and if the dehydrogenation involved in this process can only occur on carbon atoms bonded directly to the surface, then the hydrogen dependence of the fouling process should coincide with the size of the multiplets involved. The slope of the deactivation curve for the monometallic catalyst (*2*) was indicative of relatively large ensembles (sextets) being involved in fouling. But, the slope of the deactivation curve for the bimetallic catalyst (Fig. 6) is indicative of relatively small ensembles (possibly doublets) involved in the rds of fouling. Thus, it appears that the differences in hydrogen kinetics are reasonably consistent with the simple multiplet fouling model (*6*).

It is observed that the fouling activation energy for the bimetallic catalyst (Eq. (4)) is slightly greater than that observed for the monometallic catalyst (Eq. (6)). The magnitude of the difference is probably not reproducible. However, the activation energy for fouling appears to decrease by ~2 kcal/mol for each additional site involved in the rds of the fouling process (*6*). Thus, if the bimetallic catalyst is fouled by a process using smaller multiplets than the sextets proposed for the monometallic, the activation energy of the bimetallic may be up to 8 kcal greater on the basis of ensemble size alone.

SUMMARY

There are several significant differences between the main and fouling reaction kinetics of the sulfided Pt + Re/Al_2O_3 reaction system and that of the unsulfided Pt/Al_2O_3 reaction system under similar conditions. The extent of surface coverage by adsorbed toluene, the hydrogen kinetics of the fouling process, and the shape of the catalyst activity decay curve are all significantly different in these two catalyst systems. These differences suggest that the active platinum sites on this catalyst may be effectively partitioned into small ensembles of sites, presumably due to the sulfur pretreatment and the cosupported rhenium atoms as suggested by Biloen *et al.* (*10*).

APPENDIX: NOMENCLATURE

ΔE_1, ΔE_3	activation energy of k_1 and k_3
k_0, k_1, k_3	reaction rate constants for main reaction model
k_f	specific fouling rate (min^{-1})
K_2, K_x, K_y	adsorption equilibrium constants
x	moles of H_2 dissociated upon MCH adsorption
[ ]	brackets are used to signify reactor partial pressures (Torr)
r_{TOL}	rate of toluene production (mol/g · s)

ACKNOWLEDGMENTS

This work was supported in part by funds from Exxon Corporation, Proctor and Gamble Company, and from the Committee on Research of the University of California at Berkeley.

REFERENCES

1. Kluksdahl, H. E., US Patent 3,415,737 (1968).
2. Pacheco, M. A., and Petersen, E. E., *J. Catal.* **86,** 75 (1984).
3. Jossens, L. W., and Petersen, E. E., *J. Catal.* **73,** 377 (1982).
4. Jossens, L. W., and Petersen, E. E., *J. Catal.* **73,** 366 (1982).
5. Jossens, L. W., and Petersen, E. E., *J. Catal.* **76,** 265 (1982).
6. Pacheco, M. A., and Petersen, E. E., *J. Catal.* **88,** 400 (1984).
7. Andreev, A. A., Shopov, D. M., and Kiperman, S. L., *Kinet. Catal.* **7,** 941 (1966).
8. Sinfelt, J. H., Hurwitz, H., and Shulman, R. A., *J. Phys. Chem.* **64,** 1559 (1960).
9. Orozco, J. M., and Webb, G., *Appl. Catal.* **6,** 67 (1983).
10. Biloen, P. Helle, J. N., Verbeek, H., Dautzenberg, F. M., and Sachtler, W. M. H., *J. Catal.* **63,** 112 (1980).
11. Pacheco, M. A., and Petersen, E. E., *J. Catal.* **96,** 499 (1985).
12. Pacheco, M. A., Ph. D. thesis. University of California, Berkeley, 1984.